Int. J. Nanosci. Nanotechnol., Vol. 15, No. 4, Dec. 2019, pp. 229-237

Modelling of Cylindrical Contact Theories of Hertz and JKR for the Manipulation of Biological Micro/Nanoparticles

Moharam Habibnejad Korayem*, Moein Taheri, Hesam Khaksar and Rouzbeh Nouhi Hefzabad

Robotic Research Laboratory, Center of Excellence in Experimental Solid Mechanics and Dynamics, School of Mechanical Engineering, Iran University of Science and Technology, P.O. Box 13114-16846 Tehran, Iran.

(*) Corresponding author: hkorayem@iust.ac.ir
(Received: 18 February 2017 and Accepted: 18 October 2019)

Abstract

This paper deals with the development and modeling of cylindrical contact theories and also the simulation of contact forces to be applied in the manipulation of various biological micro/nanoparticles by means of the AFM. First, the simulation of contact forces in four environments has been carried out, which are the most commonly used fluid in biomanipulation. Then, the spherical and cylindrical contact models of Hertz and JKR have been compared for the nanoparticles of gold and DNA, and the developed cylindrical models have been validated by comparing the cylindrical contact results with the existing spherical contact results. The biomanipulation of rod-shaped micro/nanoparticles in different biological environments have been modeled and the results have been compared. The modeling results indicated that the JKR cylindrical model, developed in this article, had less deformation for gold nanoparticles compared with biological nanoparticles, which was justifiable in view of the considered particles' mechanical properties.

Keywords: *Nanomanipulation, Contact forces, Cylindrical contact theories, Indentation depth.*

1. INRODUCTION

Atomic Force Microscope (AFM) is an important tool for the imaging and manipulation of biological particles in liquid environments. In recent decades, many research works have been conducted on the exact modeling of nano-manipulation procedures based on the use of AFM probe as a nanomanipulator [1-5]. A new AFM-based real-time identification method is proposed for estimating the dynamic properties of proteins by Kim et al.. It provides on-line measurement of mechanical properties of proteins as well as identifying protein motions [6]. The effects of AFM cantilever stiffness on the penetration force characteristics were investigated by Kwon et al. [7].

Falvo has carried out the initial modeling of the driving of nanoparticles and the reaction forces exerted on particles; however, he has not considered surface adhesion forces in his modeling [8]. Using the JKR spherical contact theory, Tafazzoli and Sitti have presented a model [9] which simulates the dynamic behavior of a particle while it is driven on a substrate.

Korayem et al. examined the set of commonly used contact models in contact with biological particles. These models include: Hertz, DMT, JKRS, BCP, MD, COS, PT, and Sun. The group also studied contact by finite element solution [10]. Korayem et al. also investigated the effect of moisture and adhesion on the manipulation process [11]. Korayem et al. developed contact models and used finite element method to study contact mechanics of capped cylindrical nanoparticles. The results indicate that with same properties, indentation depth of

capped cylindrical nanoparticle is more than cylindrical and less than spherical geometry [12]. Since the use of nanosized continuous environment models has been greatly simplified, Korayem and his colleagues investigated the manipulation process in the molecular environment. This paper presented the Fixed Interfacial Multiscale Method (FIMM) for computationally and mathematically efficient modeling of solid structures [13].

Zhupanska explored different cases of adhesion force between a plate and cylinder. Since he had considered the friction force in his investigations, he presented a theory that was different from the JKR's [14]. Korayem et al. also investigated the contact mechanics of circular crowned roller particles. The contact models used in this study did not consider adhesive force [15].

It should be noted that the major shortcoming with most of the nano-manipulation contact models proposed in the literature is that they consider the simplest form for the studied nanoparticles, which is the spherical form. These models are not able to depict the real shapes of biological particles and therefore cannot accurately model these types of particles. Hence in this article, first, the cylindrical contact models of Hertz and JKR are developed and compared with similar spherical contact models and then these models are further developed for biological environments for the manipulation of different biological micro/nanoparticles presumed as nanorods.

2. METHODOLOGY

2.1. Effective Contact Forces in the Contact Between Two Particles

2.1.1. Van der Waals Force

The magnitude of the Van der Waals force (F_{vdw}) is obtained from the following relation using the Hamaker constant [15]:

$$F_{vdw} = \left[-A / 8\sqrt{2} D^{5/2} \right] R^2 \quad (1)$$

Where A is the Hamaker coefficient, which is a constant that depends on the material properties, D is the separation distance and R is the radius of cylindrical particle

2.1.2. Electrical Double-Layer Force

The following relations are used for the electrical double-layer zone [16]:

$$F_{el} = \kappa^{3/2} \sqrt{R/2\pi} Z e^{-\kappa D} \quad (2)$$

Where κ is the inverse of the Debye length, R is the radius of cylindrical particle, and Equation (3) gives the interaction constant Z:

$$Z = 64\pi\varepsilon\varepsilon_0 \left(K_B T / e\right)^2 \times \tanh^2\left(Ze\psi_0 / 4K_B T\right) \quad (3)$$

Where ε_0 is the vacuum permittivity, ε is the dielectric constant of the liquid, K_B is the Boltzmann constant, T is the temperature, and ψ_0 is the surface potential.

2.1.3. Hydration

The hydration force is calculated as follows [17]:

$$F(x) = C_1 \exp(-D/\lambda_H) + C_2 \exp(-D/\lambda_H) \quad (4)$$

Where $F(x)$ is the short-range force, D is the separation between the surfaces, C_1 and C_2 are hydration constants, and λ_H is the Debye length:

$$\lambda_H = \sqrt{\varepsilon\varepsilon_0 K_B T / 2Ce^2} \quad (5)$$

2.1.4. Simulation of the Effective Forces in the Contact between Two Particles

In this section, the Van der Waals force, electrical double-layer force and hydration force are simulated for four biological environments of water, 10% ethanol, 20% ethanol and methanol. As observed in the diagram of Fig. 1(a), with the increase of the distance between cylindrical nanoparticle and surface, the magnitude of Van der Waals force approaches zero. Fig. 1(b) shows the simulation of the electrical double-layer force. This diagram indicates that with the increase of the separation distance from the surface, this force also approaches zero. Fig. 1(c) illustrates the hydration force, which also approaches zero with the increase of the separation

distance. However, the clear difference between these three diagrams is that the electrical double-layer force approaches zero at a farther separation distance compared to the other two forces. This means that the electrical double-layer force enjoys a higher significance in the manipulation of cylindrical nanoparticles, followed by the hydration force and, finally, the Van der Waals force.

2.2. Theories of Cylindrical Contact Mechanics

2.2.1. Hertz Contact Model

Initial research works on the subject of contact mechanics are attributed to Hertz [18]. Hertz theory is only valid for elastic states and it does not consider adhesion forces. In this model, the relationship between contact radius and loading force is expressed as [18]:

$$F_{(adh)Hertz} = 0 \tag{6}$$

$$a_{Hertz} = 4P\bar{R}/\pi E^{*} \tag{7}$$

Where $F_{(adh)Hertz}$ is the adhesion force, a_{Hertz} is the contact radius, P is the externally applied force, $\bar{R}$ is the equivalent radius of two surfaces that have a interaction, and E^{*} is the effective modulus of elasticity, $1/E^{*}=m_t/2[(1-v_1^2)/E_1+(1-v_2^2)/E_2]$, E_1 and E_2 are the Young's moduli and v_1 and v_2 are the Poisson's ratios of the two surfaces in contact and m_t is a constant and dependent parameter on the geometry of the tip ($m_t=1$ for a cylindrical geometry, $m_t=1.5$ for spherical geometry and $m=2$ for conical forms).

In modeling, the geometry of the AFM tip was considered spherical. Moreover, the relationship between indentation depth and contact radius and also between indentation depth and applied load can be calculated by the following equations, respectively [19]:

$$\delta_{Hertz} = \left[2\ln\left(4\bar{R}/a_{Hertz}\right)-1\right]\frac{a_{Hertz}^2}{2\bar{R}} \tag{8}$$

$$\delta_{Hertz} = \left[\ln\left(\frac{4\mathrm{L}\bar{\mathrm{R}}\pi E^{*}}{\mathrm{P}}\right)-1\right]\frac{\mathrm{P}}{\mathrm{L}\pi E^{*}} \tag{9}$$

In the above relation, δ_{Hertz} is the indentation depth, P is the externally applied force, E^{*} is the effective modulus of elasticity.

In this section, since the external force P includes the main intermolecular forces such as the electrostatic force (F_{el}), steric force (F_{steric}) and the hydration force (F_{Hyd}) in addition to the externally applied dynamic force (F_1), by developing the Hertz cylindrical model for the considered biological environment, we will have:

$$P = F_1 + F_{el} + F_{steric} + F_{Hyd} \tag{10}$$

It has been demonstrated that in the absence of adhesion, the Hertz model describes the areas of contact between elastic bodies precisely.

2.2.2. JKR Contact Model

As was pointed out, the Hertz contact model doesn't take the adhesion force into consideration. For this reason, Johnson et al. [20] also studied the adhesion effect. In this model, the relationship between contact radius and loading force per unit length is expressed as [21]:

$$F_{(adh)JKR} = \left(\pi E^{*} a_{JKR}^2/4\bar{R} - \sqrt{2\pi E^{*}\omega}\right) \tag{11}$$

$$a_{JKR} = \left(2\bar{R}^2\omega/\pi E^{*}\right)^{1/3} \tag{12}$$

Where $F_{(adh)JKR}$ is the adhesion force, a_{JKR} is the contact radius, R is radius of cylindrical particle, ω is the work of the adhesion force. Also, the relationship between indentation depth and contact radius can be determined as follows [20]:

$$\delta_{JKR} = a_{JKR}^2/\bar{R} - \sqrt{8\pi\omega a_{JKR}/3E^{*}} \tag{13}$$

In the above relation, δ_{JKR} is the indentation depth. The JKR model is suitable for the modeling of reactions between probe tip and very soft samples where the adhesion force is so strong that it overcomes the stiffness of the sample and causes the surface to be pulled towards the probe tip.

2.3. Target Nanoparticles

Studies have shown that DNA can be considered as a nano-size spherical pack [22]. Therefore, a globular bundle of DNA with a diameter of 40 and gold nanoparticles with a diameter of 50 nanometer have been used in this article [9, 10].

3. RESULTS

3.1. Comparison between Spherical and Cylindrical Contacts of Gold and DNA Nanoparticles Using the Hertz Model

As noted, the total force exerted on the contact is calculated from Equation 10. For this reason, the impact of the forces must first be examined in general. As can be seen in the Fig.1, the intermolecular forces reach zero as the separation distance increases. Also, the effect of these forces is very small and in the range of a few nN.

As is observed in Fig. 2(a), for the same indentation depth created, the Hertz model indicates a smaller force for spherical gold nanoparticles than for cylindrical ones, which is predictable considering a sphere's smaller contact area relative to a cylinder's and which confirms the accuracy of the performed simulations.

Also, Fig. 2(b) illustrates the changes of contact radius with indentation depth in the Hertz contact model for the manipulation of spherical and cylindrical gold nano-particles. It is observed in Fig. 2(c) that for the same indentation depth created, the Hertz model indicates a smaller force for spherical DNA nanoparticles than for cylindrical ones. Also, Fig. 2(d) illustrates the changes of contact radius with indentation depth in the Hertz contact model for the manipulation of spherical and cylindrical DNA nanoparticles.

3.2. Comparison Between Spherical and Cylindrical Contacts of Gold and DNA Nanoparticles Using the JKR Model

As is observed in Fig. 3(a), for the same indentation depth created, the JKR model indicates a much smaller force for spherical gold nanoparticles than for cylindrical ones, which is expected considering a sphere's smaller area of contact relative to a cylinder's and also the inclusion of the adhesion force in the JKR theory.

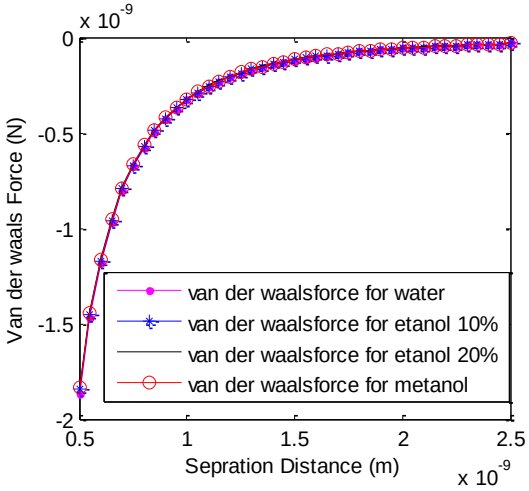

(a)

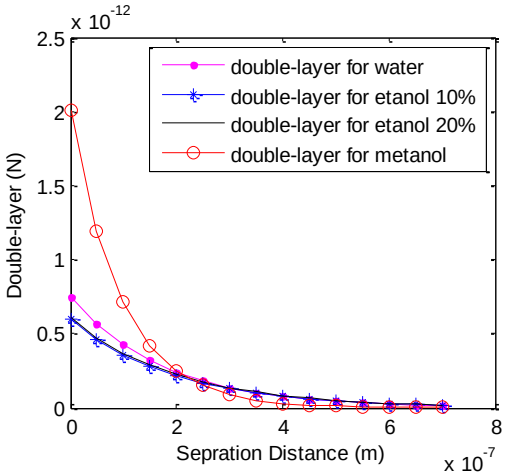

(b)

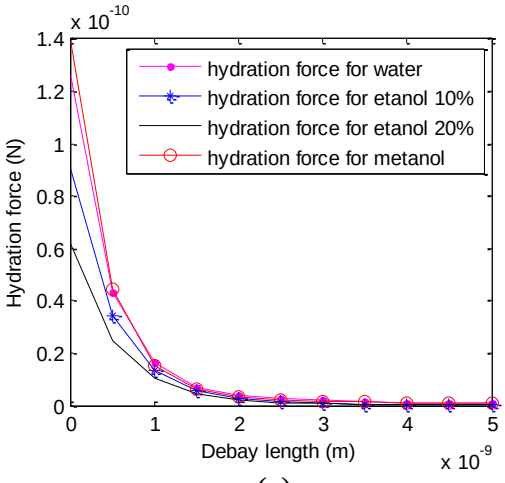

(c)

Figure 1. *Simulation of contact forces; (a) Van der Waals force, (b) Electrical double-layer force, (c) Hydration force.*

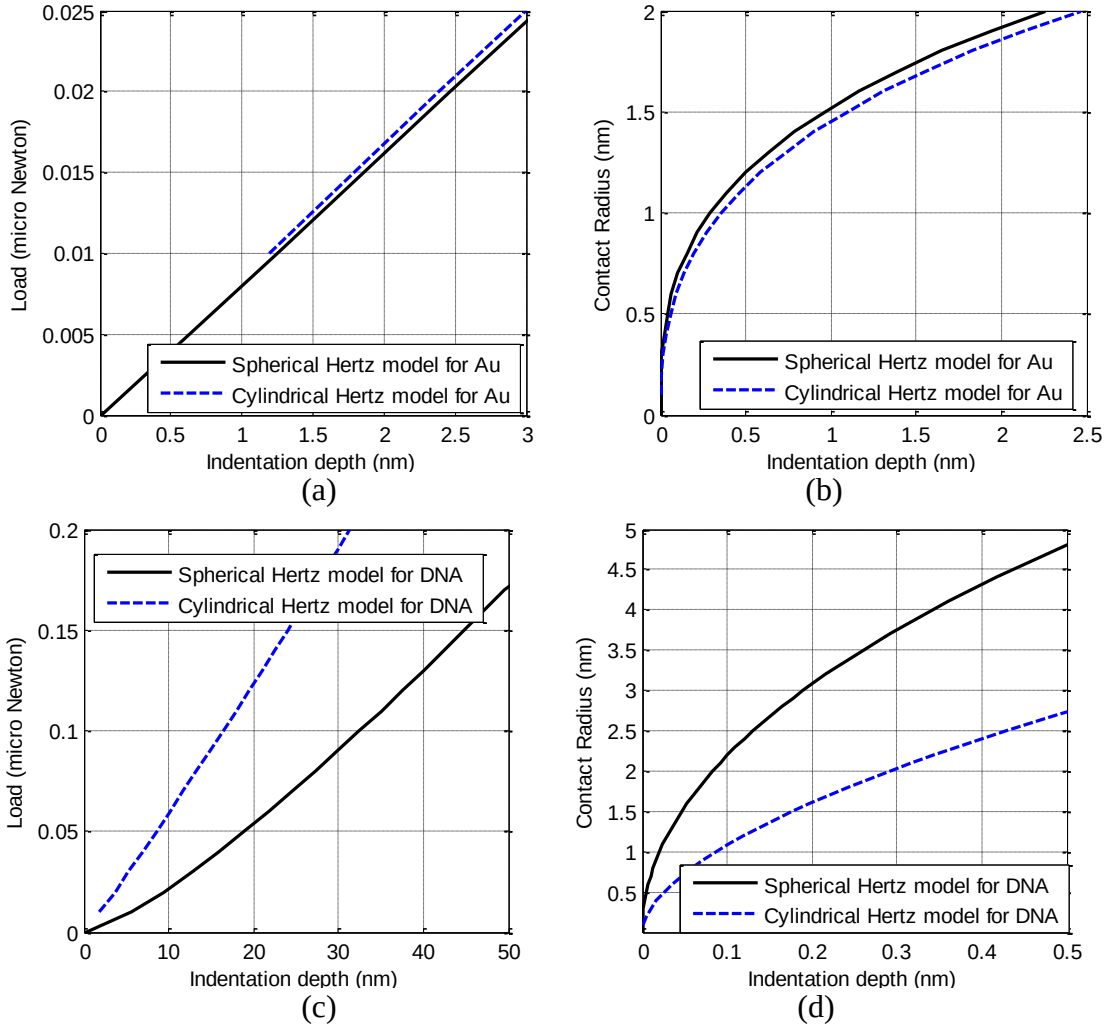

Figure 2. *Changes of force and contact radius versus indentation depth in the Hertz contact model for Au (a & b) and DNA (c & d).*

This confirms the validity of the performed simulations.

Also, Fig. 3(b) illustrates the changes of contact radius with indentation depth in the JKR contact model for the manipulation of spherical and cylindrical gold nanoparticles. This figure demonstrates that to cause the same deformation in gold nanoparticles, the spherical model needs a smaller force, which is justified in view of the contact area in this model.

It is observed in Fig. 3(c) that for the same indentation depth created, the JKR model indicates a lower magnitude force for spherical DNA nanoparticles than for cylindrical ones, which is predictable considering a sphere's smaller contact area relative to a cylinder's. Also, Fig. 3(d) shows the changes of contact radius with indentation depth in the JKR contact model for the manipulation of spherical and cylindrical DNA nanoparticles.

In view of figures (2) and (3) it can be concluded that, in general, for the same exerted force, cylindrical nanoparticles undergo less deformation compared to spherical nanoparticles, which is justifiable considering the smaller contact area in cylindrical contacts relative to spherical contacts and which confirms the validity of performed simulations.

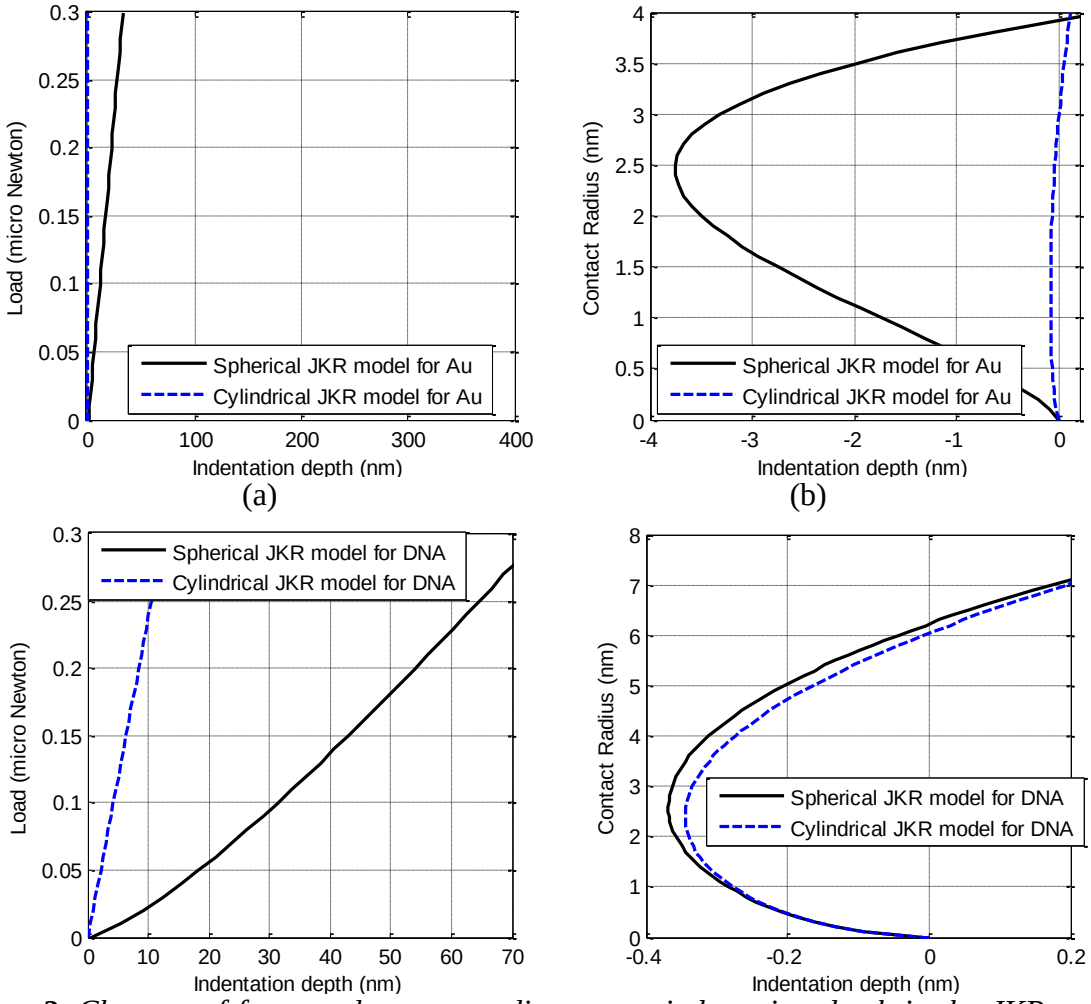

Figure 3. *Changes of force and contact radius versus indentation depth in the JKR contact model for cylindrical nanoparticles of Au (a & b) and DNA (c & d).*

3.3. Simulation of Cylindrical Contact for Different Biological Micro/Nano-particles Using the Hertz and JKR Models

In this section, we simulate the Hertz and JKR contact models for the biomanipulation of different cylindrical micro/nanoparticles including gold, DNA, yeast, platelet and nanobacterium and investigate the changes of force and contact radius with indentation depth in these contact models.

As is shown in Fig. 4(a), for the same indentation depth created, the Hertz model indicates a smaller force for biological cylindrical micro/nanoparticles than for cylindrical gold micro/nanoparticles, which is predictable considering the lower modulus of elasticity for biological particles. Fig. 4(b) shows the changes of contact radius with indentation depth in the Hertz contact model for the bio-manipulation of different cylindrical micro/nanoparticles.

As is shown in Fig. 4(c), for the same indentation depth created, the JKR model (similar to the Hertz model) indicates a smaller force for biological nanoparticles, which is justified considering the lower modulus of elasticity for biological nanoparticles. Also, Fig. 4(d) illustrates the changes of contact radius with indentation depth in the JKR contact model for different cylindrical micro/nanoparticles. It is observed from this figure that for the same indentation depth, this model (like the Hertz model) leads to less severe deformation in a gold nanoparticle compared to a biological one, which is predictable considering the fact that

biological nanoparticles have a lower modulus of elasticity.

According to this figure, most of the platelets and DNAs exhibit the same deformation under the application of load. This is similar to the simulation results of spherical contact models and it validates the presented simulations.

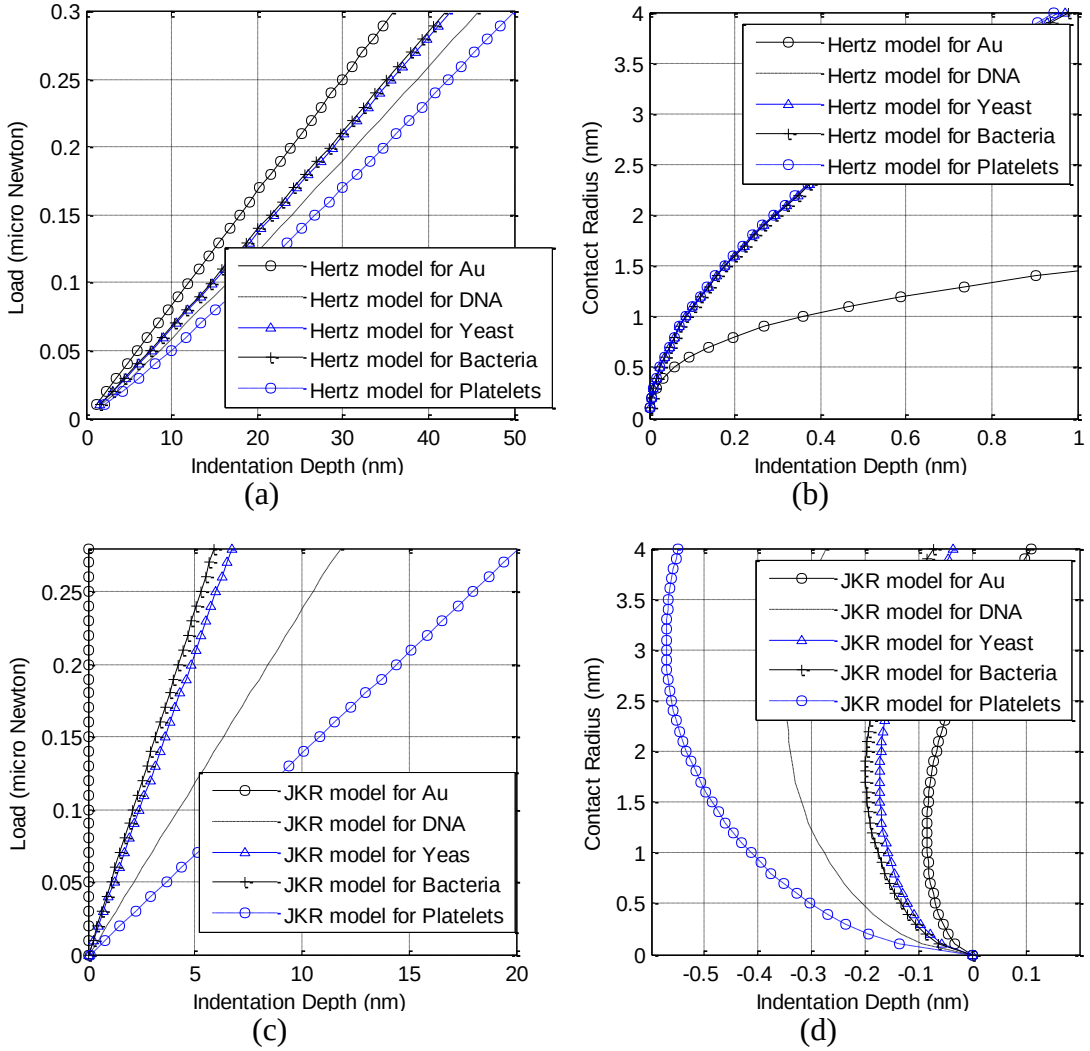

Figure 4. *Changes of force and contact radius versus indentation depth in the Hertz (a & b) and JKR (c & d) contact models for cylindrical nanoparticles.*

4. CONCLUSION

In the manipulation of biological particles, the first step of simulation is to have an exact knowledge of contact mechanics and contact forces acting between nanoparticle/probe tip and nanoparticle/substrate.

The contact forces simulated in this article indicate that with the increase of the separation distance, all three forces of Van der Waals, electrical double-layer and hydration approach zero. The important point, however, is that at closer distances, the effect of the electrical double-layer force is more than the other two forces. The developed cylindrical contact models in this article demonstrate that in general, for the same exerted force, cylindrical nanoparticles undergo less deformation compared to spherical nanoparticles. Also based on the obtained results, the use of spherical and cylindrical contact models of Hertz in analyzing the manipulation of biological nanoparticles is inappropriate and it generates considerable error, because this type of model doesn't take the adhesion force into consideration. In this article, both the developed cylindrical

contact models of Hertz and JKR indicate more deformation for gold nanoparticles compared to biological nanoparticles, which is justifiable with regards to the mechanical properties of gold and the higher elasticity modulus of gold nanoparticles. The developed contact models also indicate over 1.15 times more deformation for yeasts and nanobacteria in comparison to DNAs and platelets. This is also predictable in view of the properties considered for these nanoparticles.

Finally, it is concluded that for the precise displacement of various biological particles, it would be essential to consider the effect of different contact forces and the real shapes of the particles and to employ more exact contact models for the control of applied forces and for precise manipulation. In view of the significant role of simulation in illuminating the process of nanomanipulation, assemblage and precise displacement control of biological particles, it is necessary to study the above process with respect to particles of different shapes in addition to spherical and cylindrical forms.

REFERENCES

1. Resch, R., Bugacov, A., Baur, C., Koel, B., Madhukar, A., Will, P. (1998). "Manipulation of Nanoparticles Using Dynamic Force Microscopy: Simulation and Experiments", *Applied Physics A-Materials Science & Processing*, 67: 265-271.
2. Decossas, S., Mazen, F., Baron, T., Bremond, G., Souifi, A. (2003). "Atomic Force Microscopy Nanomanipulation of Silicon Nanocrystals for Nanodevice Fabrication", Nanotechnology, 14: 1272-1278.
3. Decossas, S., Patrone, L., Bonnot, A., Comin, F., Derivaz, M., Barski, A., Chevrier, J. (2003). "Nanomanipulation by Atomic Force Microscopy of Carbon Nanotubes on Nanostructured Surface", *Surface Science*, 543: 57-62.
4. Korayem, M. H., Hefzabad, R. N., Taheri, M., Mahmoodi, Z. (2014). "Finite Element Simulation of Contact Mechanics of Cancer Cells in Manipulation Based on Atomic Force Microscopy". *International Journal of Nanoscience and Nanotechnology*, *10*(1): 1-12.
5. Du, E., Cui, H., Zhu, Z. (2006). "Review of Nanomanipulators for Nanomanufacturing", *International Journal of Nanomanufacturing*, 1: 83-104
6. Kim, D. H., Park, J., Kim, M, K., Hong, K, S. (2008). "AFM-based identification of the dynamic properties of globular proteins: simulation study", *Journal of Mechanical Science and Technology*, 22: 2203-2212.
7. Kwon, E, Y., Kim, Y, T., Kim, D. E. (2009). "Investigation of penetration force of living cell using an atomic force microscope", *Journal of Mechanical Science and Technology*, 23, pp. 1932-1938
8. Falvo, M.R. Superfine, R. (2000). "Mechanics and Friction at the Nanometer Scale", *Journal of Nanoparticle Research*, 2: 237-248.
9. Tafazzoli, A. Sitti, M. (2004). "Dynamic Models of Nano-Particle Motion During Nanoprobe Based Nanomanipulation", *Proc. of 4th IEEE Conf. in Nanotechnology*, Germany.
10. Korayem, M. H., Rastegar, Z. (2012). "Application of Nano-Contact Mechanics Models in Manipulation of Biological Nano-Particle: FE Simulation", *International Journal of Nanoscience and Nanotechnology*, 8(1) : 35-50.
11. Korayem, M. H., Rastegar, Z., Korayem, A. H., Heidari, A. E. (2013). "Modeling of air relative humidity effect on adhesion force in manipulation of nano-particles and its application in AFM". *International Journal of Nanoscience and Nanotechnology*, 9(1): 39-50.
12. Korayem, M. H., Khaksar, H., Taheri m., (2014). "Simulating the impact between particles with applications in nanotechnology fields (identification of properties and manipulation)", *International Nano Letters*, 4: 121-127.
13. Korayem, M. H., Sadeghzadeh, S. (2012). "Dynamics of macro–nano mechanical systems; fixed interfacial multiscale method". *International Journal of Nanoscience and Nanotechnology*, 8(4): 227-246.
14. Zhupanska, O. I. (2012). "Adhesive full stick contact of a rigid cylinder with an elastic half-space", *International Journal of Engineering Science*, 55: 54-65.
15. Korayem, M. H., Khaksar, H., Taheri, M. (2013). "Modeling of contact theories for the manipulation of biological micro/nanoparticles in the form of circular crowned rollers based on the atomic force microscope", *Journal of Applied Physics*, 114(18): 183715.
16. Marina R., Israelachvili. J. N. (2008). "*Surface Forces and Nanorheology of Molecularly Thin Films*", Springer Berlin Heidelberg, Chapter 13.

17. Fabio, L. L., Carolina, C. B., Alessandra, L. R. D., Ervino C. Z., Osvaldo N. O. (2012). "Theoretical Models for Surface Forces and Adhesion and Their Measurement Using Atomic Force Microscopy", *International Journal of Molecular Sciences*, 13: 12773-12856.
18. Hertz, H. (1881). "Über die Berührung fester elastischerKörper", *Journal für die reine und angewandteMathematik*, 92: 156-171.
19. Jin, F., Guo, X. (2010). "Non-slipping adhesive contact of a rigid cylinder on an elastic power-law graded half-space", *International Journal of Solids and Structures*, 47: 1508- 1521.
20. Johnson, K. L., Kendall, K. Roberts, A. D. (1971). "Surface energy and the contact of elastic solid", *Proceedings of the Royal Society of London A*, 324: 301-313.
21. Chen, S., Wang, T. (2006). "General solution to two-dimensional nonslipping JKR model with a pulling force in an arbitrary direction", *Journal of Colloid and Interface Science*, 302: 363-369.
22. Arsuagaa, J., Tan, R. K., Vazquez, M., Sumners, D. W., Harvey, S. C. (2002). "Investigation of viral DNA packaging using molecular mechanics models", *Biophysical Chemistry*, 101: 475-484.